Resolution estimation for imaging and time reversal in scattering media

Liliana Borcea[1], George Papanicolaou[2], and Chrysoula Tsogka[3]

[1] Comput. and Applied Math., MS 134, Rice U., Houston, TX 77005-1892, USA
[2] Department of Mathematics, Stanford U., Stanford, CA 94305, USA
[3] CNRS/LMA, 31 Chemin Joseph Aiguier, 13402 Marseille cedex 20, FRANCE

Abstract. An array of transducers receives the signals emitted by a localized source in a scattering acoustic medium. The recorded signals can be used either in a time-reversal (TR) process in order to refocus acoustic energy back onto the source, or in a matched field imaging (MF) process in order to estimate the source location. In TR the signals are time-reversed and emitted into the physical medium whereas in MF they are time-reversed and back-propagated numerically in a fictitious homogeneous medium. Given the range (distance from the array) of the active source we study here the cross-range resolution in these two processes. As expected, multiple-scattering enhances the refocusing resolution in TR but it degrades resolution in the estimation of the source location with MF. We introduce a robust procedure for *estimating* the resolution gain (resp. loss) in TR (resp. MF), in weakly scattering random media. Direct numerical simulations in the ultrasound regime show that our estimation method is accurate and effective.

1 Time reversal and imaging in a scattering medium

A point source located at $\boldsymbol{y}$ emits a signal $s_0(t)$ which is received by a linear array of point transducers located at $\boldsymbol{x}_p = (ph/2, 0, 0)$, for $p = -N, \dots N$, as shown in Fig. 1. The range and direction (bearing) of the source with respect to the array, as seen from the central element $\boldsymbol{x}_0$, are $\mid \boldsymbol{y} - \boldsymbol{x}_0 \mid = L$ and α, respectively. The signals received by the transducer located at $\boldsymbol{x}_p$ have the form

$$s_p(t) = s_0(t) \star G(\boldsymbol{x}_p, \boldsymbol{y}, t) = \frac{1}{2\pi} \int_{-\infty}^{\infty} \hat{s}_0(\omega) \hat{G}(\boldsymbol{x}_p, \boldsymbol{y}, \omega) e^{-i\omega t} d\omega. \tag{1}$$

Here $\hat{s}_0(\omega)$ and $\hat{G}(\boldsymbol{x}_p, \boldsymbol{y}, \omega)$ are the Fourier transforms of the pulse and the two point Green's function at frequency ω, respectively, and $\star$ denotes convolution in time. The time harmonic Green's function $\hat{G}$ satisfies the reduced wave equation

$$\Delta \hat{G}(\boldsymbol{x}, \boldsymbol{y}, \omega) + k^2 n^2(\boldsymbol{x}) \hat{G}(\boldsymbol{x}, \boldsymbol{y}, \omega) = -\delta(\mathbf{x} - \boldsymbol{y}), \tag{2}$$

where $k = \omega/c_0$ is the wavenumber, c_0 is a reference speed of propagation and $n(\boldsymbol{x}) = c_0/c(\boldsymbol{x})$ is the index of refraction of the medium with local propagation speed $c(\boldsymbol{x})$. At infinity, $\hat{G}$ satisfies a Sommerfeld radiation condition.

In *Time Reversal* (TR), the signals $s_p(t)$, received at the array are recorded, time reversed and re-emitted into the actual mediumi. In *Imaging* (IM), the

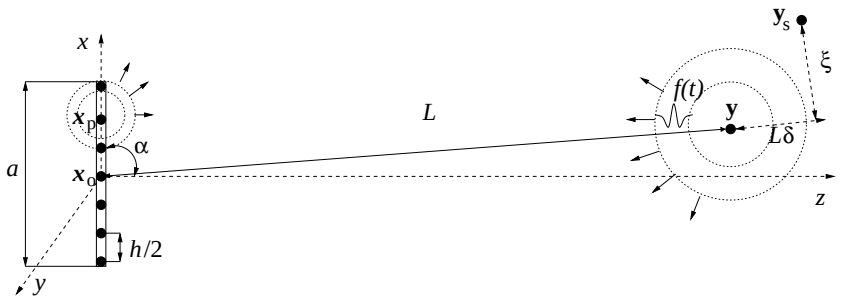

Fig. 1. The array, active source setup for time reversal and imaging

recorded signals $s_p(t)$, are time reversed and back-propagated numerically in a *homogeneous* medium. In either case we consider the back-propagated field at a "search" point $\boldsymbol{y}_s$ as shown in Fig. 1. We take $\boldsymbol{y}_s$ in the plane determined by $\boldsymbol{y}$ and the array, at range $\eta = L(1+\delta)$ and cross-range ξ.

The time-reversed and back-propagated field at the search point, is given by

$$I^{TR}(\boldsymbol{y}, \boldsymbol{y}_s, t) = \frac{1}{2\pi} \int_{-\infty}^{\infty} e^{-i\omega t} \hat{I}^{TR}(\boldsymbol{y}, \boldsymbol{y}_s, \omega), \tag{3}$$

where

$$\hat{I}^{TR}(\boldsymbol{y}, \boldsymbol{y}_s, \omega) = \overline{\hat{s}_0(\omega)} \sum_{p=-N}^{N} \overline{\hat{G}(\boldsymbol{x}_p, \boldsymbol{y}, \omega)} \hat{G}(\boldsymbol{x}_p, \boldsymbol{y}_s, \omega). \tag{4}$$

For imaging, the Fourier transform of the field at the search point, is given by

$$\hat{I}^{IM}(\boldsymbol{y}, \boldsymbol{y}_s, \omega) = \overline{\hat{s}_0(\omega)} \sum_{p=-N}^{N} \overline{\hat{G}(\boldsymbol{x}_p, \boldsymbol{y}, \omega)} \hat{G}_0(\boldsymbol{x}_p, \boldsymbol{y}_s, \omega), \tag{5}$$

where $\hat{G}_0(\boldsymbol{x}_p, \boldsymbol{y}_s, \omega)$ is the Green's function of the reduced wave equation in a homogeneous medium, given by (7). It is well known that refocusing for time reversal is tighter in random media than in homogeneous ones because of multiple scattering [2,6,4]. Moreover, this statistical enhancement of the refocusing is stable in the time domain but not in the frequency domain [2,8]. By stable we mean here that the refocused field is self-averaging, hence close to deterministic, in the time domain, in a suitable remote sensing and multiple scattering regime. On the other hand, refocusing for imaging is wider in random media than in homogeneous ones because multiple scattering impedes the identification of the source location.

For imaging the cross-range of the source we use the autocorrelation or matched field (MF) of the back-propagated field at zero lag

$$I^{MF}(\boldsymbol{y}_s) = \int_{-\infty}^{\infty} |\hat{I}^{IM}(\boldsymbol{y}, \boldsymbol{y}_s, \omega)|^2 d\omega. \tag{6}$$

The matched field functional is also self-averaging, hence statistically stable, and provides an estimate of the cross-range of the source. The range must, however, be estimated separately from arrival time information. Various functionals for imaging the location of an active source and their relative performance are considered in [3]. Our main result in this paper is an analytical formula for the matched field functional $\Gamma^{MF}(\boldsymbol{y}_s)$ that can be used to estimate an unknown **effective aperture** a_e when the range is known (e.g., from arrival time analysis). This estimation is very important because it permits both assessing quantitatively super-resolution in time reversal and estimating the loss of cross-range resolution in imaging by the matched field method.

2 The mathematical model

For homogeneous media the Green's function of the reduced wave equation is,

$$\hat{G}_0(\boldsymbol{x},\boldsymbol{y},\omega) = \frac{e^{ik|\boldsymbol{x}-\boldsymbol{y}|}}{4\pi|\boldsymbol{x}-\boldsymbol{y}|}\ , \quad k=\frac{\omega}{c_0}, \tag{7}$$

in three dimensions, whereas in two dimensions, $\hat{G}_0$ is given by a Hankel function of the first kind. For simplicity, our analytical calculations are done in three dimensions. In the numerical simulations, however, we solve the 2D acoustic wave equation in the time domain. For the spatial discretization we use a finite element method [1] and for the time discretization we use a centered second order finite difference scheme. Although the numerical calculations are two dimensional, our analytical results can be applied, since only the phase (not the amplitude) of the Green's functions is important in the analysis.

For the scattering medium, we assume a statistically homogeneous, Gaussian random velocity field, with constant mean $c_0 = 1.5$km/s, correlation length $l = 0.3$mm and standard deviation ranging from 1% to 5%. While the velocity fluctuations are sufficiently small such that imaging is still possible, we ensure that there is significant multipathing in the medium by taking $\lambda_0 \sim l \ll a \ll L$. The pulse used in the numerical simulations, is given by

$$s_0(t) = \frac{dg(t)}{dt},\ g(t) = \frac{1}{\sqrt{2\pi\sigma_t^2}} e^{-i\omega_0 t} e^{-\frac{t^2}{2\sigma_t^2}}, \tag{8}$$

with $\sigma_t = 0.2325\mu$s and central frequency $2\pi\omega_0 = 3$MHz (i.e. $\lambda_0 = 0.5$mm). The aperture of the array is $a = 2.5$mm and $L = 2$cm.

2.1 Time reversal in random media

The time reversed, back-propagated field in the random medium is given by (3). Because of the statistical stability of $\Gamma^{\mathrm{TR}}(\boldsymbol{y}_s,t)$ (cf. [2,8]), it is close to its expectation, denoted by $<\cdot>$. Using the moment formula [5,7] and assuming that $a \ll L$, $\xi = O(a)$ and $\delta \ll 1$, we get

$$\left\langle \overline{\hat{G}(\boldsymbol{x}_p,\boldsymbol{y};\omega)}\hat{G}(\mathbf{x}_p,\boldsymbol{y}_s;\omega)\right\rangle \approx \overline{\hat{G}_0(\mathbf{x}_p,\boldsymbol{y};\omega)}\hat{G}_0(\boldsymbol{x}_p,\boldsymbol{y}_s;\omega) e^{-\frac{k^2\xi^2 a_e^2}{2L^2}}, \tag{9}$$

where a_e is an unknown parameter that we interpret as an effective aperture for the array. To analyze the refocusing of the time reversed, back-propagated field, we calculate $\hat{I}^{\rm TR}$ at points on a fictitious screen at the correct range L ($\delta = 0$). Given the pulse (8), we obtain

$$I^{\rm TR}(\xi, L; t) \approx \frac{a}{8\pi^2 L^2 h} \int \frac{\sin\left(\frac{\omega a \sin\alpha \xi}{2c_0 L}\right)}{\frac{a\sin\alpha\xi}{2c_0 L}} e^{-\frac{\sigma_t^2(\omega-\omega_0)^2}{2} - \frac{\omega^2\xi^2 a_e^2}{2c_0^2 L^2} - i\omega\left(t - \frac{\xi^2}{2c_0 L}\right)} d\omega. \tag{10}$$

After integrating with respect to ω and evaluating the field at the arrival time $t = \xi^2/2c_0 L$, we get for $\xi \ll \sigma_t c_0 L/a_e$,

$$I^{\rm TR}(\xi, L; \frac{\xi^2}{2c_0 L}) \approx \frac{c_0}{4\pi^2 L h \xi \sin\alpha} \frac{-i}{\sqrt{2\pi\sigma_t^2}} \sin\left(\frac{\omega_0 \xi a \sin\alpha}{2c_0 L}\right) e^{-\frac{A^2\xi^2}{8c_0^2 L^2 \sigma_t^2}}, \tag{11}$$

where

$$A^2 = a^2 \sin^2\alpha + 4\omega_0^2 \sigma_t^2 a_e^2. \tag{12}$$

With a similar calculation in deterministic media we obtain

$$I_0^{\rm TR}(\xi, L; \frac{\xi^2}{2c_0 L}) \approx \frac{c_0}{4\pi^2 L h \xi \sin\alpha} \frac{-i}{\sqrt{2\pi\sigma_t^2}} \sin\left(\frac{\omega_0 \xi a \sin\alpha}{2c_0 L}\right) e^{-\frac{a^2\sin^2\alpha\xi^2}{8c_0^2 L^2\sigma_t^2}}. \tag{13}$$

Comparing (11) and (13) we note that the physical apparent aperture in homogeneous media ($a\sin\alpha$) is replaced by a larger apparent aperture ($A \geq a\sin\alpha$) in random media, which explains the super-resolution. Note also, that (12) implies that the bandwidth of the pulse, expressed by $\omega_0\sigma_t$, plays an important role in refocusing: for a given random medium, the apparent aperture of the array increases as the bandwidth decreases, and thus better refocusing is obtained. However, the bandwidth cannot be too small because at some point statistical stability breaks down. We note here that a_e is the key parameter in estimating the apparent aperture and consequently the refocusing in random media. The estimation of this parameter is carried out in the next section.

2.2 Estimation of a_e using Matched Field in random media

The matched field functional is given by (6), which in the frequency domain is,

$$\hat{I}^{\rm MF}(\boldsymbol{y}_S; \omega) = |\hat{s}_0(\omega)|^2 \sum_{p,q=-N}^{N} \overline{\hat{G}_0(\boldsymbol{x}_p, \boldsymbol{y}_s; \omega)} G(\mathbf{x}_p, \boldsymbol{y}; \omega) \overline{\hat{G}(\boldsymbol{x}_q, \boldsymbol{y}; \omega)} G_0(\boldsymbol{x}_q, \boldsymbol{y}_s; \omega). \tag{14}$$

Because of the statistical stability of $\int \hat{I}^{\rm MF}(\boldsymbol{y}_S; \omega) d\omega$, we can take the expectation in the right hand side of (14) and using the moment formula (cf. [5,7]) we get

$$\left\langle \overline{\hat{G}(\boldsymbol{x}_p, \boldsymbol{y}; \omega)} \hat{G}(\mathbf{x}_q, \boldsymbol{y}; \omega) \right\rangle \approx \overline{\hat{G}_0(\mathbf{x}_p, \boldsymbol{y}; \omega)} \hat{G}_0(\boldsymbol{x}_q, \boldsymbol{y}; \omega) e^{-\frac{k^2 a_e^2}{2L^2} |\boldsymbol{x}_p - \boldsymbol{x}_q|^2 \sin^2\alpha}. \tag{15}$$

Plugging (15) into (14) and after some calculations we obtain

$$\hat{\Gamma}^{\mathrm{MF}}(\xi,\eta;\omega) \approx \frac{4aL\lambda\left|\hat{s}_0(\omega)\right|^2}{\sqrt{2\pi}h^2 a_e \sin\alpha(4\pi L)^4}\; e^{-\frac{\xi^2}{2\eta^2}\left(\frac{L}{a_e}\right)^2}, \tag{16}$$

Comparing (16) with (11) we note that the parameter a_e plays the opposite role in imaging than it does in time-reversal. Indeed, a larger effective aperture a_e, leads to resolution loss in imaging while it enhances resolution in time-reversal.

To confirm the statistical stability of the matched field we show in Fig. 2 the quantity $\Gamma^{\mathrm{MF}}(\boldsymbol{y}_s)$ computed numerically for two realizations of the random medium. By matching this numerically computed field to the theoretical prediction given by (16) we get an estimate of a_e. Its estimated values for four realizations of the random medium are 1.43, 1.54, 1.37, 1.46 (in mm). Using now the mean value of a_e (1.45mm) we calculate from (10) the theoretically predicted time-reversed field. We show in Fig. 2 this theoretically predicted field as well as the numerically calculated ones for two of the realizations of the random medium. The enhanced refocusing in the random medium is seen clearly, as is the very good agreement between the theoretical prediction and the numerical simulations.

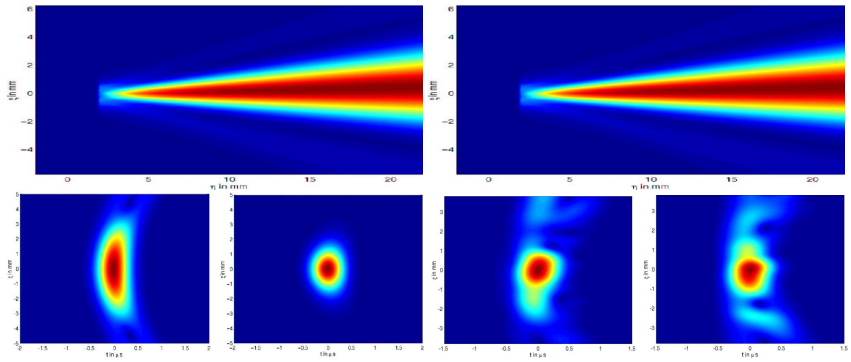

Fig. 2. Top: $\Gamma^{\mathrm{MF}}(\boldsymbol{y}_s)$ computed numerically for two realizations of the random medium, the estimation of a_e is 1.43mm (resp. 1.47mm) for the data on the left (resp. right). Bottom (left to right): the theoretical prediction of the time-reversal field in a homogeneous medium, in a random medium obtained using $a_e = 1.45$mm in (10) and the numerically calculated time-reversal field for two realizations of the random medium.

References

1. E. Bécache, P. Joly, C. Tsogka: SIAM J. Numer. Anal., **37** (2000)
2. P. Blomgren, G. Papanicolaou, H. Zhao: J. Acoust. Soc. Am. **111** (2002)

3. L. Borcea, G. Papanicolaou, C. Tsogka, J. Berryman: Inverse Problems, **18** (2002)
4. A. Derode, P. Roux, M. Fink: Phys. Rev Letters, **75** (1995)
5. A. Ishimaru, *Wave Propagation and Scattering in Random Media* (Academic Press, New York, 1978)
6. M. Fink: Scientific American, **281** (1999)
7. D. R. Jackson and D. R. Dowling: J. Acoust. Soc. Am. **89**, (1991)
8. G. Papanicolaou, L. Ryzhik, K. Solna: SIAM J. on App. Math. (subm. 2002)